



Structure and thermal properties of stearic acid/silica composites as form-stable phase change materials

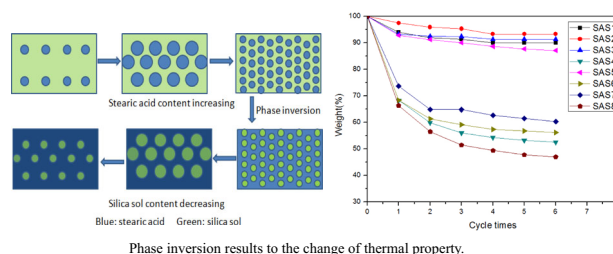
Zhenjin Fu¹ · Li Dai¹ · Yong Yi¹ · Jiangshan Luo² · Bo Li²

Received: 21 May 2018 / Accepted: 13 July 2018 / Published online: 21 July 2018
© Springer Science+Business Media, LLC, part of Springer Nature 2018

Abstract

In this study, stearic acid/silica phase change composites were prepared by the sol-gel method using stearic acid as phase change materials (PCMs). The effects of mass fraction of stearic acid were comprehensively investigated. The structures and thermal properties of the obtained composites were characterized by various methods, including scanning electron microscopy (SEM), differential scanning calorimetry (DSC), leakage tests, and thermogravimetry analysis (TG). The results indicated that composite containing 76% stearic acid had the best thermal properties and low mass leakage, making 76% stearic acid as the maximum content that silica matrix could protect in the composites. The latter was further confirmed by morphological analyses of the silica matrix. Silica matrix exhibited spherical particle clusters, following big–small–big–small size pattern as stearic acid rose. The composite with 76% stearic acid was at the key point of change in particle size. These findings look promising for future to prepare silica-based phase change composites with good thermal properties easily.

Graphical Abstract



Highlights

- The composite containing 76% stearic acid showed good thermal properties.
- Silica particle size changed with stearic acid content in composites.
- The composite with 76% stearic acid was at the key point of change in particle size.

Keywords Stearic acid · Silica · Structure · Phase change composites · Thermal property

✉ Zhenjin Fu
zhenjin18@126.com

✉ Jiangshan Luo
jiangshanluo@caep.cn

✉ Bo Li
LB6711@126.com

¹ School of Materials Science and Engineering, Southwest University of Science and Technology, Mianyang 621010, China

² Research Center of Laser Fusion, China Academy of Engineering Physics, Mianyang 621900, China

1 Introduction

Phase change materials (PCMs) can absorb or release large amounts of latent heat. Hence, they are often used as heat storage materials for different purposes such as seasonal energy storage, thermo-regulated textile, and energy-saving building materials [1–4]. PCMs are usually divided into two kinds from chemical composition: organic and inorganic PCMs [1]. Organic PCMs, such as paraffin, polyethylene glycol (PEG) and fatty acids are the most commonly used materials due to their suitable melting temperatures, high energy storage abilities, and chemical inertness [5, 6]. Among investigated organic PCMs, paraffin and fatty acids have attracted increasing interest due to their low cost. However, leakage during thermal cycling limits their usage since this decreases the effective enthalpy and shortens lifetime of the material [7]. Therefore, numerous form-stable PCM composites and encapsulated PCMs have been investigated to overcome the leakage issue [7–10].

Silica [11, 12], expanded graphite [13, 14], Kaolin [15], diatomite [16], and gypsum [3] are used as support materials in form-stable PCM composites for their porous structure. PCMs are embedded in the support materials by different means, including sol-gel [17–22], vacuum adsorption [14, 23], and polymerization [24, 25]. By vacuum adsorption method, the mass of PCMs adsorbed into support materials relies on the support materials pores volume. It is hard to increase the mass of adsorbed PCMs under this limitation. But there are more possibilities to change the pore structure in composites by using sol-gel and polymerization methods. Therefore, silica-based phase change composites are synthesized by mature sol-gel technology [17–22]. On the other hand, in this process, silica sol is first mixed with different PCMs to embed them in the silica framework after gelation, which is simple and easy to do [26]. Silica is one of the components of building materials, and silica-based PCMs composites materials could be given priority in building heat-regulating materials [27].

However, the properties of form-stable PCM composites and the appropriate mass content of PCMs in composites are different with the same sol-gel method. Ma et al. [21] synthesized lauric acid/silica composites using maximum mass of lauric acid of 69.1%. And lauric acid was uniformly imbedded into silicon dioxide without melted leakage from the composites. Li et al. [19] prepared paraffin/SiO₂ composites by the sol-gel method using maximum mass content of paraffin of 53.5%, with latent heat 112.8 kJ/kg. Silicone gel was formed and paraffin was dispersed in the porous network. Fang et al. [20] prepared palmitic acid/SiO₂ composite with latent heat 85.11 kJ/kg. The maximum mass percentage of palmitic acid in the composites was estimated to 41.1%, and the leakage of composites may occur with the increasing mass of palmitic acid. Li et al. [22] prepared the

shape-stabilized paraffin/silicon dioxide composite by using sol-gel method. The maximum mass percentage of paraffin dispersed into the composites was up to 92.1%, and there was no leakage of the paraffin from the composites.

In this view, several studies reported silica-based PCMs composites with relevant properties and the maximum PCMs content, the causes behind the results were rarely discussed. So it is especially important to discover the rule of formation process in preparing silica-based phase change composites. In our previous study, silica-based phase change composites containing organic PCMs of stearic acid, paraffin and polyethylene glycol were prepared by the sol-gel process [8]. During gelation, the three PCMs made the pore size of silica framework different. And this led to different thermal properties of the composites. Among them, the prepared stearic acid/silica composites showed good thermal properties. Therefore, a further and systematic research about stearic acid/silica composites should be proceeded to discover the rule of form-stable process.

In this study, several stearic acid/silica phase change composites were prepared using the sol-gel method. The maximum mass content of stearic acid present in PCM composites, leakage tests, and silica structure were examined. The relationship between thermal properties of the composites and silica structure, and the formation of silica structure in composites were explained.

2 Experimental

2.1 Materials

Tetraethyl silicate (TEOS, Analytical Reagent) was purchased from Tianjin Kemiou Chemical Reagent, China. Stearic acid (CH₃(CH₂)₁₆COOH, Analytical Reagent) was obtained from Guangzhou Jinhua Chemical Reagent, China. Hydrochloric acid (HCl, Analytical Reagent, 36–38wt.%), ammonium hydroxide (NH₃·H₂O, Analytical Reagent, 28 wt.%) and ethanol (CH₃CH₂OH, Analytical Reagent, Chengdu Institute of Chemical Reagents, China) were used as received without further purification. Deionized water was used for preparation of all aqueous phases.

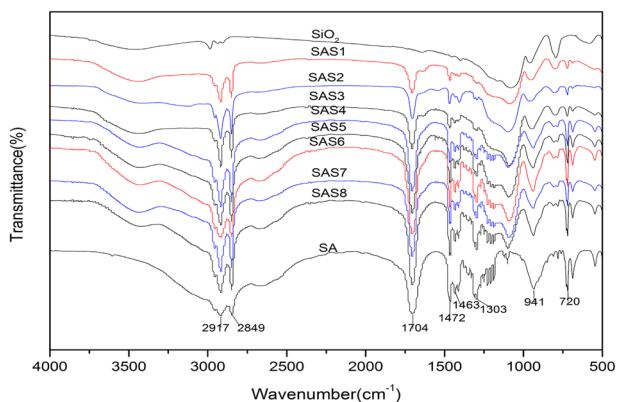
2.2 Composite preparation

First, silica sol was prepared by the following procedure: TEOS (60 mL), ethanol (120 mL) and distilled water (0.5 mL) were mixed in a 500 mL flask under magnetic stirring. Next, hydrochloric acid was added as catalyst and pH of the mixture was adjusted to 1–2. The mixture was then kept at 60 °C for 6 h to obtain the silica sol.

Second, phase change composites were prepared by the following route: silica sol (4.5 g) and ethanol (4 g) were

Table 1 The content of stearic acid and silica in SAS composites

Samples	SAS1	SAS2	SAS3	SAS4	SAS5	SAS6	SAS7	SAS8
Stearic acid	38%	56%	61%	69%	76%	79%	81%	85%
Silica	62%	46%	39%	31%	24%	21%	19%	15%

**Fig. 1** FTIR spectra of SiO₂, stearic acid and SAS composites

mixed with stearic acid (1, 2, 2.5, 3.5, 5, 6, 7, and 9 g) in respective beakers. Ammonium hydroxide was then added to the mixture. After stirring at 800 rpm in water bath for 0.5 h at 60 °C, gels were obtained. Next, the composite gels were dried at 80 °C for 24 h to yield stearic acid/silica composites. The composites were ground in an agate mortar and marked as SAS1, SAS2, SAS3, SAS4, SAS5, SAS6, SAS7 and SAS8, corresponding to stearic acid contents of 38, 56, 61, 69, 76, 79, 81 and 85%, respectively. And the content of stearic acid and silica in SAS composites were showed in Table 1.

2.3 Characterization

The phase change properties in terms of melting/freezing points and latent heats were obtained by differential scanning calorimetry (DSC, TA, Q-100) from 25 to 70 °C at heating/cooling rate of 5 °C min⁻¹ under argon atmosphere. The chemical compositions of SAS composites were tested by Fourier transform Infrared (FTIR, Nicolet iS5) spectroscopy. The morphologies were characterized by scanning electron microscopy (SEM, Hitachi TM-3000). The thermal stabilities of SAS composites were obtained by a thermogravimetry analyzer (TG, TA Q-500) at the scanning rate of 10 °C min⁻¹, temperature range of 50–600 °C, and under argon atmosphere.

The leakage tests could provide information on changes in composite thermal properties. The composites were first weighed then placed on filter paper. After heating at 80 °C for 20 min followed by cooling to room temperature, the composites were weighed again and mass loss was calculated. Next, the composites were placed on other filter papers to run other thermal cycles. The above procedure

was performed consecutively until mass loss was close to zero.

3 Results and discussion

3.1 Chemical characterization of composites

Figure 1 shows the FTIR spectra of stearic acid, SiO₂, and prepared SAS composites with various mass fractions of stearic acid. The spectrum of pure SiO₂ revealed extra peaks at 1079 cm⁻¹ and 795 cm⁻¹, assigned to asymmetric and symmetric stretching vibration of Si–O–Si group, respectively. The broad peak at 3436 cm⁻¹ was attributed to bending vibration of Si–OH. The peaks at 2917 cm⁻¹ and 2849 cm⁻¹ in the spectrum of stearic acid originated from C–H stretching vibrations of methyl and methylene groups, respectively. The peaks at 1472 cm⁻¹ and 1463 cm⁻¹ were attributed to bending vibrations of methylene group, and those at 1704 cm⁻¹ and 1303 cm⁻¹ corresponded to stretching vibrations and in-plane bending vibrations of C=O group and –OH, respectively. Overall, all the characteristic peaks of stearic acid and SiO₂ were present in spectra of the composites. Also, no new peaks appeared in spectra of the composites, indicating the physical mixture of stearic acid and SiO₂ during gelation of silica sol.

3.2 Thermal properties of composites

3.2.1 DSC analysis

Figure 2 illustrates the DSC curves of stearic acid and SAS composites. The heat absorption and release properties of the composites and stearic acid are listed in Table 2. The latent heat values of the composites were compared to those of stearic acid, and the effective PCM mass percentage in the composites was calculated by Eq. (1),

$$\text{PCM}(\%) = (\Delta H_{\text{composites}} / \Delta H_{\text{stearic acid}}) \times 100, \quad (1)$$

where $\Delta H_{\text{composites}}$ and $\Delta H_{\text{stearic acid}}$ (170.3 J g⁻¹) are the melting enthalpies of the composites and pure stearic acid measured by DSC, respectively.

As can be seen in Fig. 2, all composites exhibited the endothermic and exothermic peaks of stearic acid. As mass fraction of stearic acid rose in the composites, the endothermic and exothermic peak intensities strengthened.

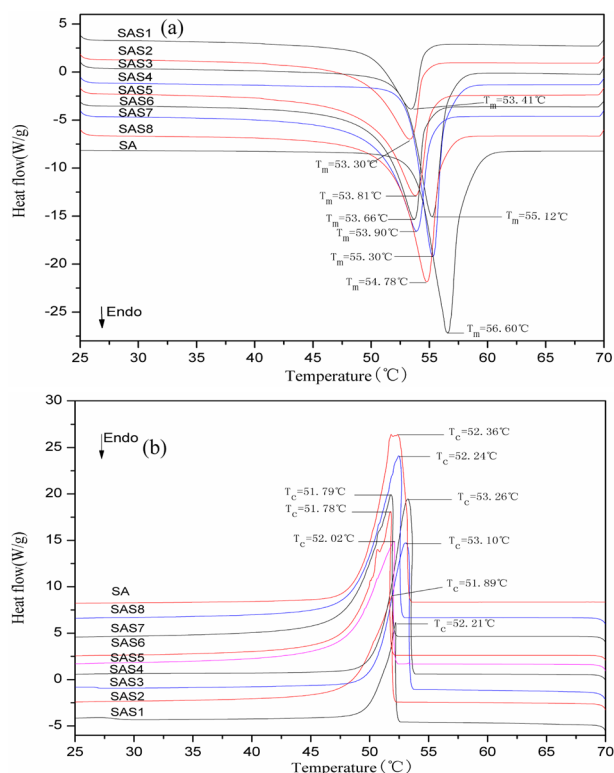


Fig. 2 DSC thermograms of stearic acid and SAS composites (a) melting process; (b) crystallization process

Table 2 DSC data of stearic acid and SAS composites

Samples	ΔH_m (J·g ⁻¹)	T_m (°C)	ΔH_c (J·g ⁻¹)	T_c (°C)	$ePCM\%$	$tPCM\%$
SA	170.3	56.60	170.7	52.36	100	100
SAS1	52.19	53.41	49.06	52.21	30.65	38
SAS2	82.83	53.30	83.19	51.89	48.64	56
SAS3	115.1	55.12	103.1	53.10	68	61
SAS4	123.4	55.30	122.6	53.26	72.46	69
SAS5	118.3	53.81	117.6	52.02	69.47	76
SAS6	129.2	53.66	128.7	51.78	75.87	79
SAS7	135.7	53.90	135.5	51.79	79.68	81
SAS8	149.3	54.78	148.5	52.24	87.67	85

T_m peak temperature on DSC heating curve, T_c peak temperature on DSC cooling curve, ΔH_m melting enthalpy, ΔH_c crystallization enthalpy, $ePCM\%$ effective stearic acid content calculated by equation (1), $tPCM$ theoretical stearic acid content

Figure 2a estimated the melting temperature of SAS composites between 53.30 °C and 55.30 °C. A reduction in melting temperature of SAS composites ranging from 1.3 to 3.3 °C was noticed when compared to pure stearic acid. The most of effective stearic acid content calculated by Eq. (1) was below theoretical stearic acid content, except for SAS3,

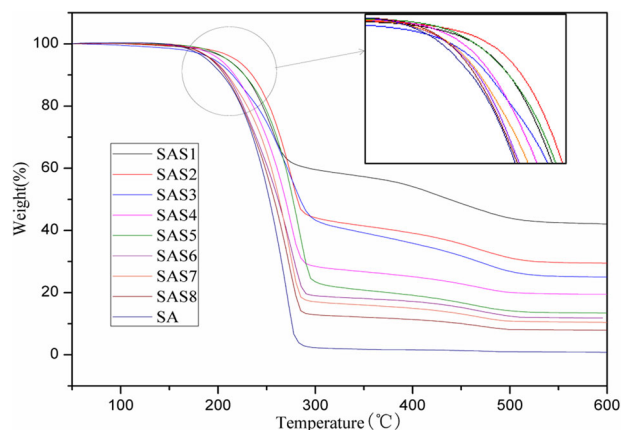


Fig. 3 TG thermograms of stearic acid and SAS composites (the inset shows amplification onset weight loss)

SAS4, and SAS8 in Table 2. The reduction in the effective PCM mass percentage was caused by confinement effect of silica mesopores [8, 21, 28]. And Schmidt et al. [29] offered the existence of “a nonfreezing layer”, which acted physically as part of the pore wall, to decrease the latent heat [30]. However, increment in effective PCM mass percentage would be an interesting phenomenon to study. These findings may indicate that thermal enthalpy of stearic acid in the composites was affected by silica structure.

3.2.2 TG testing

The thermal stabilities of stearic acid and SAS composites were evaluated by TG analysis and the results are gathered in Fig. 3. A one-step mass loss of pure stearic acid was observed, with onset weight loss temperature of 180 °C. By comparison, two-step mass losses were recorded for SAS composites. From 200 °C to 300 °C, the mass loss in SAS composites was caused by vaporization of stearic acid. From 300 °C to 500 °C, the mass loss was linked to water loss from further gelatinization. The inset revealed that onset weight loss of SAS composites shifted to high temperatures, especially for SAS1, SAS2, and SAS5. Obviously, the thermal stability of SAS1, SAS2 and SAS5 composites enhanced more than the other SAS composites. Under the action of surface tension and capillary force, the vaporization temperature of stearic acid was retarded. When stearic acid content was below 76%, the effect of capillary force was more significant.

3.2.3 Leakage testing

Leakage testing of the composites would provide information related to effect of composite content on thermal stability. Figure 4 shows photos of the composites after the first thermal treatment. Leakage of stearic acid can clearly

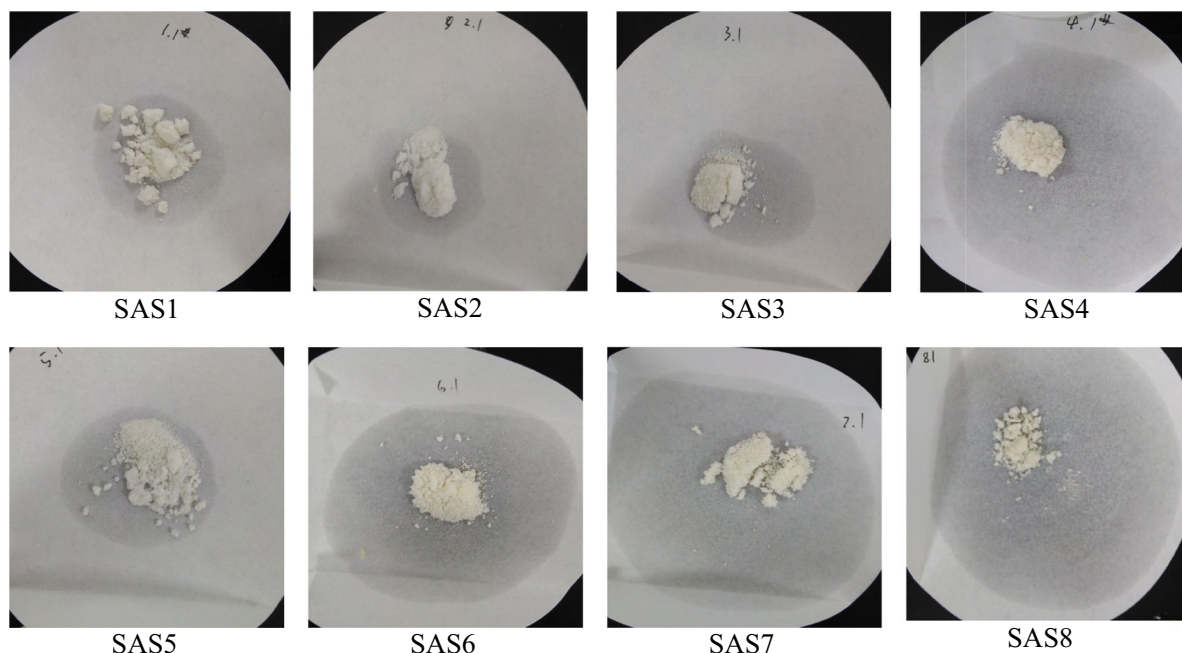


Fig. 4 Photos of SAS composites after first heat treatment

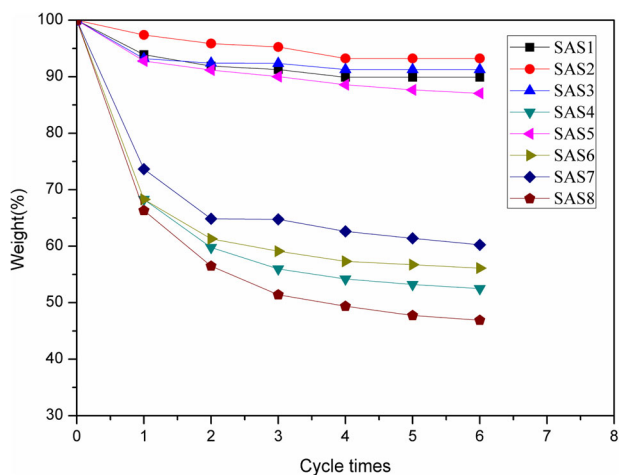


Fig. 5 The mass loss of SAS composites after every thermal cycle

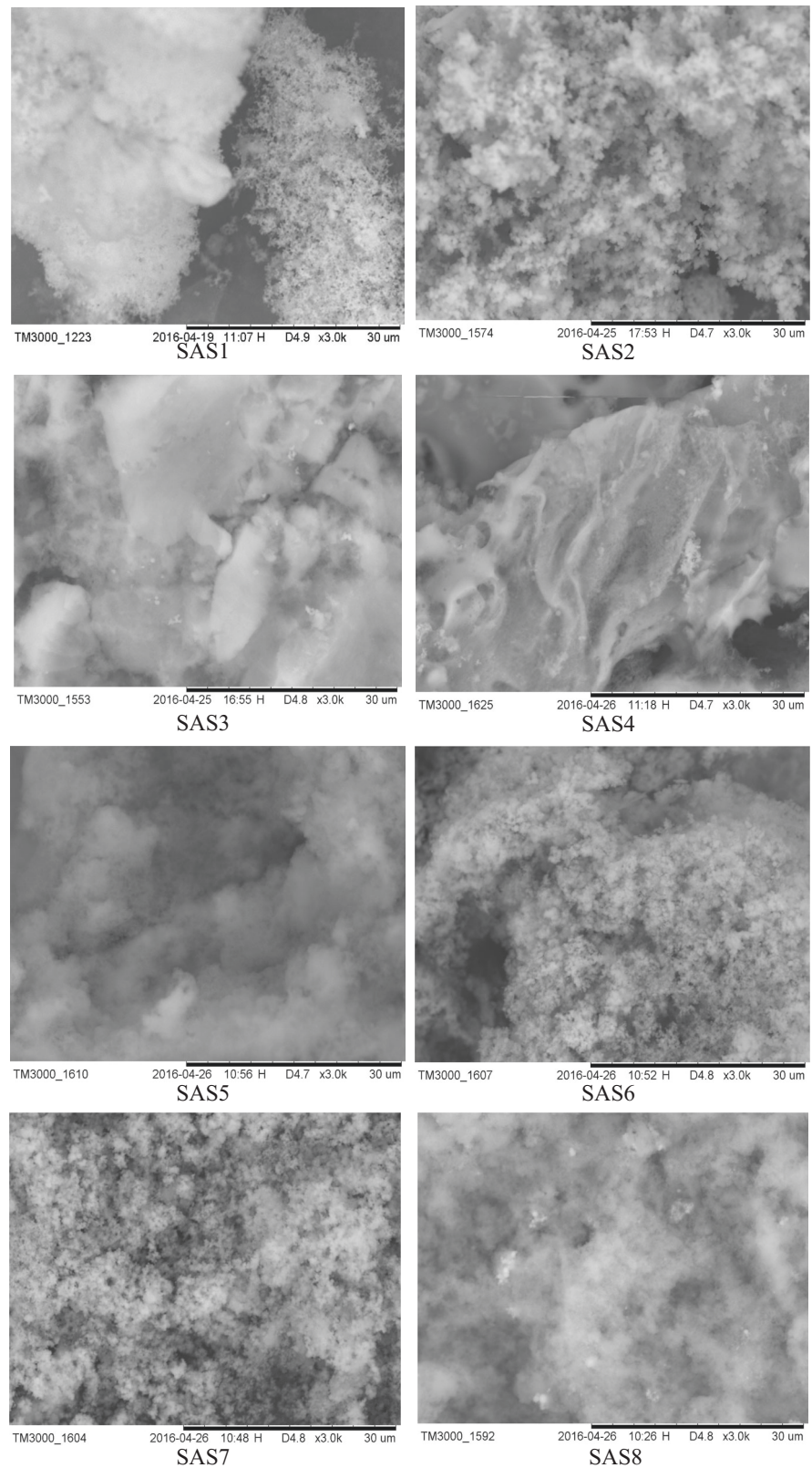
be seen from the filter paper but leakage mass among samples differed. And Fig. 5 depicts the mass loss rate of SAS composites after each thermal cycle. SAS1, SAS2, SAS3 and SAS5 composites showed gentle variation trends, with total mass losses of less than 10%. However, SAS4, SAS6, SAS7 and SAS8 illustrated distinct changes, with total mass losses exceeding 40%. As stearic acid content rose in the composites, the mass loss increased quickly after SAS5 (76% stearic acid). That was to say stearic acid content was near 76%, which was the maximum content that silica matrix could protect in the composites.

3.3 Morphology of silica in composites

The stearic acid present in the composites was extracted by ethanol for more than three times, until stearic acid could no longer be detected in silica matrix by FTIR spectroscopy. The remaining structure of silica was analyzed by SEM and the results are depicted in Fig. 6. The silica matrix exhibited spherical particle clusters with different sizes. The spherical particle sizes followed the pattern big–small–big–small as stearic acid content rose. On the other hand, as stearic acid increased, the spherical particle size of silica for both SAS1 to SAS5 and SAS6 to SAS8 reduced but the decreasing trends were not continuous. SAS5 was shown at the inflection point of change in particle size. Obviously, the gelation morphology of silica was influenced by stearic acid content in the mixed solution, and 76% stearic acid content was at the critical point of change in particle size.

Based on the above results, the change in silica morphology is shown in Fig. 7. At low contents of stearic acid solutions, stearic acid acted as dispersed phase and silica sol as continuous phase in the mixed solution. The formation of mixed solution was broken at stearic acid contents near 76% (SAS5). In other words, phase inversion occurred for stearic acid contents up to 76%, and stearic acid changed from dispersion phase to continuous phase. Therefore, the spherical particle size of silica decreased as stearic acid rose at contents below 76%. After phase inversion, the spherical particle size of silica changed to form new point. The change in morphology of continuous or dispersion phases

Fig. 6 SEM images of the silica matrix of composites after being extracted by ethanol



as a function of content were widely investigated in emulsion [31, 32]. With the increment of dispersion phase, the particle size of dispersion phase became large and

incomplete phase inversion was achieved through the coalescence [32]. And their morphology change trends were similar to the change of silica morphology. But near the

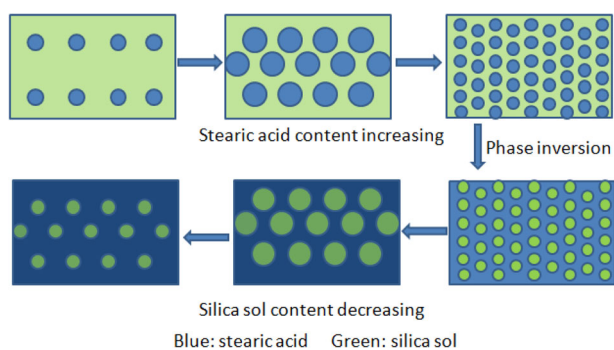


Fig. 7 Silica sol morphology in different mixed solution

phase inversion, the silica morphology became complex, which led to anomalous properties of SAS4 composite such as the increment in effective PCM mass percentage and mass loss exceeding 40% of SAS4. And Fig. 7 showed one of the most common processes of phase inversion.

Compared to TG data and leakage tests, SAS5 showed good thermal properties and low mass leakage. This indicated that stearic acid acted as dispersion phase, which would benefit the thermal properties of the composites in mixed solution. Near the point of phase inversion, the maximum content of stearic acid in composites was reached. This represented the maximum content of stearic acid, which silica matrix could embed and protect.

4 Conclusions

Stearic acid was used as PCM for thermal energy storage. Stearic acid/silica composites were prepared by the sol-gel method. The chemical properties, thermal characteristics and morphology of silica in the composites were studied. The FTIR spectral confirmed the chemical composition of SAS composites. The DSC results showed that thermal enthalpy of stearic acid in the composites was affected by silica content, and the most of effective stearic acid content was below theoretical stearic acid content. Leakage tests revealed the composites with low leakage at stearic acid mass contents below 76%, except for SAS4 composite. After extraction of stearic acid from the composites, silica matrix exhibited spherical particle clusters, following big–small–big–small size pattern as stearic acid rose. From structure viewpoint, a point of phase inversion of mixed solution probably occurred as stearic acid content rose, and near phase inversion stearic acid in composites reached maximum content at 76%, maximum content that the silica matrix could protect. The structure of SAS composites was different before and after phase inversion, which would be a key factor to affect the composites thermal properties.

Acknowledgements We would like to thank the Fund of Longshan academic talent research supporting program of SWUST (17LZXT04), and the Fund of Doctoral Program of SWUST (17zx7130).

Compliance with ethical standards

Conflict of interest The authors declare that they have no conflict of interest.

References

- Zalba B, Marin JM, Cabeza LF, Mehling H (2003) Review on thermal energy storage with phase change: materials, heat transfer analysis and applications. *Appl Therm Eng* 23:251–283
- He F, Wang X, Wu D (2015) Phase-change characteristics and thermal performance of form-stable n-alkanes/silica composite phase change materials fabricated by sodium silicate precursor. *Renew Energy* 74:689–698
- Karaipekli A, Sar A, Biçer A (2016) Thermal regulating performance of gypsum/(C18-C24) composite phase change material (CPCM) for building energy storage applications. *Appl Therm Eng* 107:55–62
- Jin W, Darkwa J, Kokogiannakis G (2017) Development of microencapsulated phase change material for solar thermal energy storage. *Appl Therm Eng* 112:1205–1212
- Sánchez P, Sánchez-Fernández MV, Romero A, Rodríguez JF, Sánchez-Silva L (2010) Development of thermo-regulating textiles using paraffin wax microcapsules. *Thermochim Acta* 498:16–21
- Jin Z, Wang Y, Liu J, Yang Z (2008) Synthesis and properties of paraffin capsules as phase change materials. *Polym (Guildf)* 49:2903–2910
- Yang D, Shi S, Xiong L et al. (2016) Paraffin/Palygorskite composite phase change materials for thermal energy storage. *Sol Energy Mat. Sol Cells* 144:228–234
- Fu Z, Su L, Liu M, Li J, Li J, Zhang Z, Li B (2016) Confinement effect of silica mesopores on thermal behavior of phase change composites. *J Sol-Gel Sci Technol* 80:180–188
- Zhang H, Wang X, Wu D (2010) Silica encapsulation of n-octadecane via sol-gel process: A novel microencapsulated phase-change material with enhanced thermal conductivity and performance. *J Colloid Interface Sci* 343:246–255
- Cao L, Tang Y, Fang G (2015) Preparation and properties of shape-stabilized phase change materials based on fatty acid eutectics and cellulose composites for thermal energy storage. *Energy* 80:98–103
- Luo R, Wang S, Wang T, Zhu C, Nomura T, Akiyama T (2015) Fabrication of paraffin@ SiO₂ shape-stabilized composite phase change material via chemical precipitation method for building energy conservation. *Energy Build* 108:373–380
- He L, Li J, Zhou C, Zhu H, Cao X, Tang B (2014) Phase change characteristics of shape-stabilized PEG/SiO₂ composites using calcium chloride-assisted and temperature-assisted sol gel method. *Sol Energy* 103:448–455
- Zhang Q, Wang H, Ling Z, Fang X, Zhang Z (2015) RT100/expand graphite composite phase change material with excellent structure stability, photo-thermal performance and good thermal reliability. *Sol Energy Mat. Sol Cells* 140:158–166
- Zhang Z, Shi G, Wang S, Fang X, Liu X (2013) Thermal energy storage cement mortar containing n-octadecane/expanded graphite composite phase change material. *Renew Energy* 50:670–675
- Memon SA, Lo TY, Shi X, Barbhuiya S, Cui H (2013) Preparation, characterization and thermal properties of Lauryl alcohol/

- Kaolin as novel form-stable composite phase change material for thermal energy storage in buildings. *Appl Therm Eng* 59:336–347
16. Kenisarin MM, Kenisarina KM (2012) Form-stable phase change materials for thermal energy storage. *Renew Sust Energy Rev* 16:1999–2040
 17. Ma F, Zong X, Chen M, Li Y (2010) Preparation and properties of lauric acid/SiO₂ phase change energy storage composite materials. *J Mat Eng* 4:15–17
 18. Qian T, Li J, Ma H, Yang J (2015) The preparation of a green shape-stabilized composite phase change material of polyethylene glycol/SiO₂ with enhanced thermal performance based on oil shale ash via temperature-assisted sol–gel method. *Sol Energy Mat. Sol Cells* 132:29–39
 19. Li M, Wu Z, Tan J (2012) Properties of form-stable paraffin/silicon dioxide/expanded graphite phase change composites prepared by sol-gel method. *Appl Energy* 92:456–461
 20. Fang G, Li H, Chen Z, Liu X (2011) Preparation and properties of palmitic acid/SiO₂ composites with flame retardant as thermal energy storage materials. *Sol Energy Mat. Sol Cells* 95:1875–1881
 21. Yang H, Feng L, Wang C, Zhao W, Li X (2012) Confinement effect of SiO₂ framework on phase change of PEG in shape-stabilized PEG/SiO₂ composites. *Eur Polym J* 48:803–810
 22. Li H, Fang G, Liu X (2010) Synthesis of shape-stabilized paraffin/silicon dioxide composites as phase change material for thermal energy storage. *J Mater Sci* 45:1672–1676
 23. Zong X, Cai Y, Sun G, Zhao Y, Huang F, Song L, Hu Y, Fong H, Wei Q (2015) Fabrication and characterization of electrospun SiO₂ nanofibers absorbed with fatty acid eutectics for thermal energy storage/retrieval. *Sol Energy Mater Sol Cells* 132:183–190
 24. Zhang Y, Wang L, Tang B, Lu R, Zhang S (2016) Form-stable phase change materials with high phase change enthalpy from the composite of paraffin and cross-linking phase change structure. *Appl Energy* 184:241–246
 25. Sari A (2004) Form-stable paraffin/high density polyethylene composites as solid-liquid phase change material for thermal energy storage: preparation and thermal properties. *Energy Convers Manag* 45:2033–2042
 26. Guo X, Zhang Q, Ding X, Shen Q, Wu C, Zhang L, Yang H (2016) Synthesis and application of several sol–gel-derived materials via sol–gel process combining with other technologies: a review. *J Sol-Gel Sci Technol* 79:328–358
 27. Jeong SG, Jeon J, Cha J, Kim J, Kim S (2013) Preparation and evaluation of thermal enhanced silica fume by incorporating organic PCM, for application to concrete. *Energy Build* 62:190–195
 28. Jackson CL, McKenna GB (1990) The melting behavior of organic materials confined in porous solids. *J Chem Phys* 93:9002
 29. Schmidt R, Hansen EW, Stoecker M, Akporiaye D, Ellestad OH (1995) Pore size determination of MCM-51 mesoporous materials by means of ¹HNMR spectroscopy, N₂ adsorption, and HREM. a preliminary study. *J Am Chem Soc* 117:4049–4056
 30. Nomura T, Zhu C, Sheng N, Tabuchi K, Sagara A, Akiyama T (2015) Shape-stabilized phase change composite by impregnation of octadecane into mesoporous SiO₂. *Sol Energy Mater Sol Cells* 143:424–429
 31. Yang Z, Zhao D, Xu M, Xu Y (1997) Analysis of the waterborne particles of bisphenol a type epoxy resin. *Chem J Chin Univ* 18:1568–1570
 32. Zhu Y, Yang Z, Zhao D (2000) The morphological evolution of water droplets during incomplete phase inversion process. *Acta Polym Sin* 4:514–517